Instrumental system to estimate the turbuce ratio of the air flow in a rigid grid, based on its reduced dynamic order transfer functions matrix

Sistema instrumental para estimar la relación de turbulencia del flujo de aire en una cuadrícula rígida, en función de su matriz de funciones de transferencia de orden dinámico reducido

Ana Marell Arteaga Martínez[1,2], Eloy Edmundo Rodríguez Vázquez[1,3], María Elizabeth Rodríguez Ibarra[1,2], Helen Janeth Zúñiga Osorio[3], Luis Álvaro Montoya Santiyanes[2,4]

[1]Engineering Center for Industrial Development (CIDESI), National Laboratory for Cooling Technology Research (LaNITeF), Av. Pie de la Cuesta 207, Desarrollo San Pablo, Querétaro, 76250 México.
[2]Universidad TecMilenio, Fudamental Science Department, Camino Real a Humilpan, Corregidora, Querétaro.
[3]Universidad Anáhuac Querétaro, School of Engineering, Quantitative Methods and Fundamental Science, Circuito Universidades, El Marques, Querétaro.
[4]Universidad Politécnica de Querétaro, School of Engineering, Carretera a los Cues, El Marques, Querétaro.

Corresponding author: Dr. Eloy Edmundo Rodríguez Vázquez, Engineering Center for Industrial Development (CIDESI), National Laboratory for Cooling Technology Research (LaNITeF), Av. Pie de la Cuesta 207, Desarrollo San Pablo, Querétaro, 76250 México. E-mail: eloy.rodriguez@cidesi.edu.mx

Abstract. – *In words of the cooling technology experts, there is at least a 20-year gap between the nowadays vapor compression based technology for refrigeration, cooling and HVAC, and what we have defined as alternatives technologies. There is also a big amount of scientific effort to endow this vapor compression technology with more degrees of freedom to implement more accurate energy optimization algorithms. In this way, as a first step to get more robust control algorithms in heat interchangers of condenser and evaporators units, authors have developed some instrumentation systems to analyze the behavior of the air flowing through the rigid blades of this kind of devices. This previous effort has been before reported as a complete vibrational modal model for the concerned rigid grid, however; due to its 16 spatially degrees of freedom and its 16th dynamic order, its model re-solution on line while the heat interchanger unit is working is almost impossible with a normal computer. Therefore, to get an algorithm with less computational resource consumption and with the same accuracy than the complete modal model, authors have reported in this document, the implementation of a reduced dynamical order transfer function matrix model. Reduction that as well as it is described is based on the poles averaging and zeros selection, from the set experimental graphs of the frequency spectral magnitude from a set of impact tests (experimental modal testing) performed at LaNITeF-CIDESI. Numerical prediction of the transfer function matrix from the dynamic reduced order*

model have been validated with the experimental spectral. Based on the hypothesis, that due to the incident angle, the resonance spectral vibration is excited by the laminar air flow, while the air flow turbulence does not excite the resonance vibrational spectral, the turbulence ration from the incident air flow has been analyzed from a wind tunnel test. As the main conclusion, authors have developed and validated a new instrumentation system to analyze the turbulence ratio of the air flow incident in a rigid grid, which can be part of a condenser or evaporator unit from a conventional cooling system, by implementing the concerned transfer functions matrix model with reduced dynamic order.

Keywords: Vibrational modal model; Laminar and turbulent air flow; Reduce order transfer functions matrix.

Resumen. - En palabras de los expertos en tecnología de enfriamiento, hay al menos una brecha de 20 años entre la tecnología actual basada en compresión de vapor para refrigeración, enfriamiento y HVAC, y lo que hemos definido como tecnologías alternativas. También hay una gran cantidad de esfuerzo científico para dotar a esta tecnología de compresión de vapor con más grados de libertad para implementar algoritmos de optimización de energía más precisos. De esta manera, como primer paso para obtener algoritmos de control más robustos en intercambiadores de calor de unidades de condensadores y evaporadores, los autores han desarrollado algunos sistemas de instrumentación para analizar el comportamiento del aire que fluye a través de las cuchillas rígidas de este tipo de dispositivos. Sin embargo, este esfuerzo anterior se informó anteriormente como un modelo modal vibracional completo para la grilla rígida en cuestión; Debido a sus 16 grados de libertad espacial y su 16 ° orden dinámico, su redisolución de modelo en línea mientras la unidad de intercambiador de calor está funcionando es casi imposible con una computadora normal. Por lo tanto, para obtener un algoritmo con menos consumo de recursos computacionales y con la misma precisión que el modelo modal completo, los autores han informado en este documento, la implementación de un modelo de matriz de función de transferencia de orden dinámico reducido. Reducción que, como se describe, se basa en el promedio de los polos y la selección de ceros, a partir de los gráficos experimentales establecidos de la magnitud espectral de frecuencia de un conjunto de pruebas de impacto (prueba modal experimental) realizadas en LaNITeF-CIDESI. La predicción numérica de la matriz de la función de transferencia del modelo dinámico de orden reducido se ha validado con el espectro experimental. Según la hipótesis, que debido al ángulo incidente, la vibración espectral de resonancia es excitada por el flujo de aire laminar, mientras que la turbulencia del flujo de aire no excita la espectral vibracional de resonancia, la relación de turbulencia del flujo de aire incidente se ha analizado desde un prueba de túnel de viento. Como conclusión principal, los autores han desarrollado y validado un nuevo sistema de instrumentación para analizar la relación de turbulencia del flujo de aire incidente en una red rígida, que puede ser parte de una unidad de condensador o evaporador de un sistema de enfriamiento convencional, mediante la implementación de la transferencia correspondiente. modelo matricial de funciones con orden dinámico reducido.

Palabras clave: Modelo modal vibracional; Flujo de aire laminar y turbulento; Reduzca la matriz de funciones de transferencia de orden.

1.   Introduction

Several international engineer organizations and company clusters like ASHRAE (American Society for Heating, Refrigeration and Air Conditioning Engineers) and ANFIR (National Association for the Refrigeration Industry Manufactures in Mexico) have reported that the perishable product preservation consumes almost 25% of electric energy [1], therefore; based on the average efficiency reported from the equipment use for the cold chain conservation, in 2016 almost 1 TWh was wasted, magnitude that represents 1,300.00 Million of USD per hour [2].

The cooling technology expert's predictions say that there is at least a 20 years' gap for the commercial consolidation of a new alternative technology for the perishables preservation. Based on this scenario, there is still a big importance to perform several researching efforts focused on the optimization of the conventional technology for refrigeration and air conditioning based on vapor compression [3 – 5].

In this point, several scientific and technological works have taken place to increase the energetic performance of these conventional cooling systems. Some of them are concentrated on the development and implementation of new materials for the thermal isolation of cooling chambers [6, 7]. Important improvements have also been reported in the alternative cooling technology development field. These developments include the regulation of different physical phenomena, as well as: thermo-acoustics [8], magneto-caloric properties [9] or arrangements of electro-thermal devices [10]. However, as it has been reported and as the experts have predicted, these alternative technologies have not achieved the same thermal load and time response capacity than the actual systems based on the vapor compression refrigeration cycle do [11, 12].

In the same way, to improve the energetic performance of the conventional cooling technology, the control engineering has been involved by trying several strategies, such as: neural networks [13], fuzzy logic [14], or adaptive linear controllers [15 - 18]. All these control algorithms are based on the compressor activation regulation, since there is only one degree of freedom that the conventional cooling technology has for the regulation of its energetic performance.

In order to get more accurate energetic optimization strategies for the conventional cooling systems, heat interchange from the condenser and evaporator units takes importance [17 - 21]. Here is where the scientific proposal of this work is grounded, because it represents the first stage to develop a control algorithm to regulate the heat interchange by monitoring the waveform magnitude from the air flowing in between of the heat interchangers blades with not affection to its thermodynamic performance.

In the next section the fundamentals of the scientific proposal are described by showing the mathematical model hypothesis and its structure. The third section shows the experimental details and the test results for the dynamic characterization of the experimental setup. Finally, in sections four and five the experimental results are analyzed and the conclusions are supported based on these results.

2.   Dynamic model fundamentals

The proposal for the waveform magnitude estimation for the air flowing through a rigid grid of a heat interchanger unit is based on the vibrational modal model from the set of blades shown on Fig. 1 which is grounded on the lumped mass structure illustrated on Fig. 2. This model has been structured based on the lumped mass hypothesis, and its coefficients come from an experimental modal test, performed at the LaNITeF facilities at CIDESI Querétaro.

The main hypothesis of this proposal is grounded on the strong correlation between the dynamic performance of the air flow in the blades and their vibrational behavior. The purpose of this effort is to know how this correlation can be monitored with an acceptable certainty.

Authors have reported the concerned model for this vibrational structure in its complete

version with a recursive adjustment of its damping coefficients [17]. That version has been considered complete because its dynamical order (16th) is the same than the spatial degrees of freedom [16].

Figure 1. Set of blades used to get the vibrational modal model.
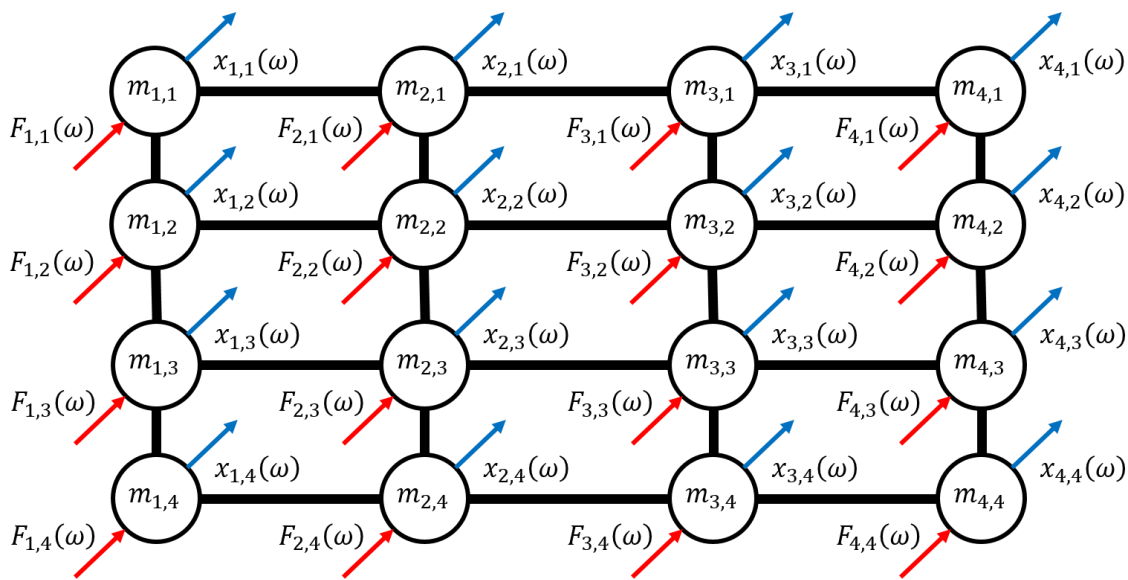
Figure 2. Structural hypothesis for the vibrational modal model.

Due to the computational resources needed to perform this model solution on line while

the heat interchanger are working, the 16 degrees of freedom with their 16th

dynamical order is not technologically feasible without a supercomputer behind. Then, authors propose the reduction of the 16 complete dynamical orders to the ones needed depending on the frequency spectral magnitude from their corresponded transfer function. Effort that is documented here.

At the end, the fundamental mathematical structure based on the lumped mass hypothesis gives the dynamic relationship between the forces $F_{n,m}$ and the output displacements $x_{a,b}$ defined by a transfer matrix, given by:

$$\begin{bmatrix} x_{1,1}(\omega) \\ x_{1,2}(\omega) \\ \vdots \\ x_{4,3}(\omega) \\ x_{4,4}(\omega) \end{bmatrix} = \frac{1}{P(\omega)} \begin{bmatrix} Z_{(1,1),(1,1)} & Z_{(1,1),(1,2)} & \cdots & Z_{(1,1),(4,3)} & Z_{(1,1),(4,4)} \\ Z_{(1,2),(1,1)} & Z_{(1,2),(1,2)} & \cdots & Z_{(1,2),(4,3)} & Z_{(1,2),(4,4)} \\ \vdots & \vdots & \ddots & \vdots & \vdots \\ Z_{(4,3),(1,1)} & Z_{(4,3),(1,2)} & \cdots & Z_{(4,3),(4,3)} & Z_{(4,3),(4,4)} \\ Z_{(4,4),(1,1)} & Z_{(4,4),(1,2)} & \cdots & Z_{(4,4),(4,3)} & Z_{(4,4),(4,4)} \end{bmatrix} \begin{bmatrix} F_{1,1}(\omega) \\ F_{1,2}(\omega) \\ \vdots \\ F_{4,3}(\omega) \\ F_{4,4}(\omega) \end{bmatrix} \quad (1)$$

where:

$P(\omega)$ is the polynomial of Eigenvalues (poles) of the entire system, and $Z_{(a,b),(n,m)} = f(\omega)$ is the polynomial of zeros that links the output variable $x_{a,b}$ with the input variable $F_{n,m}$.

For the reduced dynamical order model, the zeros polynomial order are less than 16, which again it is the most important difference between this reduced model and the complete model, and which avoids over consumption of computational resources for the model solution on line.

3. Experimental characterization of the vibrational model

Both, poles confirmation and zeros location for each transfer function between the output variables $x_{a,b}$ versus the input variables $F_{n,m}$, given by

$$G_{(a,b),(n,m)}(\omega) = \frac{Z_{(a,b),(n,m)}(\omega)}{P(\omega)} = \frac{x_{a,b}(\omega)}{F_{n,m}(\omega)} \quad (2)$$

were graphically identified from the experimental plot of the concerned variables behavior, while a set of impact tests were performed as the fundamental part of the experimental modal test. Fig. 3 shows the impact test setup where the accelerometers and instrumented hammer used are identified.

Figure 3. Experimental setup for the impact test.

Table 1 list the technical characteristics of the equipment used for the impact test experimentation.

Table 1. Technical characteristics of the equipment used.

Description	Accuracy	Model	Manufactured
Accelerometer	10.5 mV/g	*M353B17*	PCB
Instrumented Hammer	2.25 mV/N	086C03	
Data Acquisition System	NI cDAQ 9178		National Instruments
Signal Conditioning	NI 9234		

The spectral responses from some transfer functions from their 256 set of them, are shown on Figs. 4 to 7.
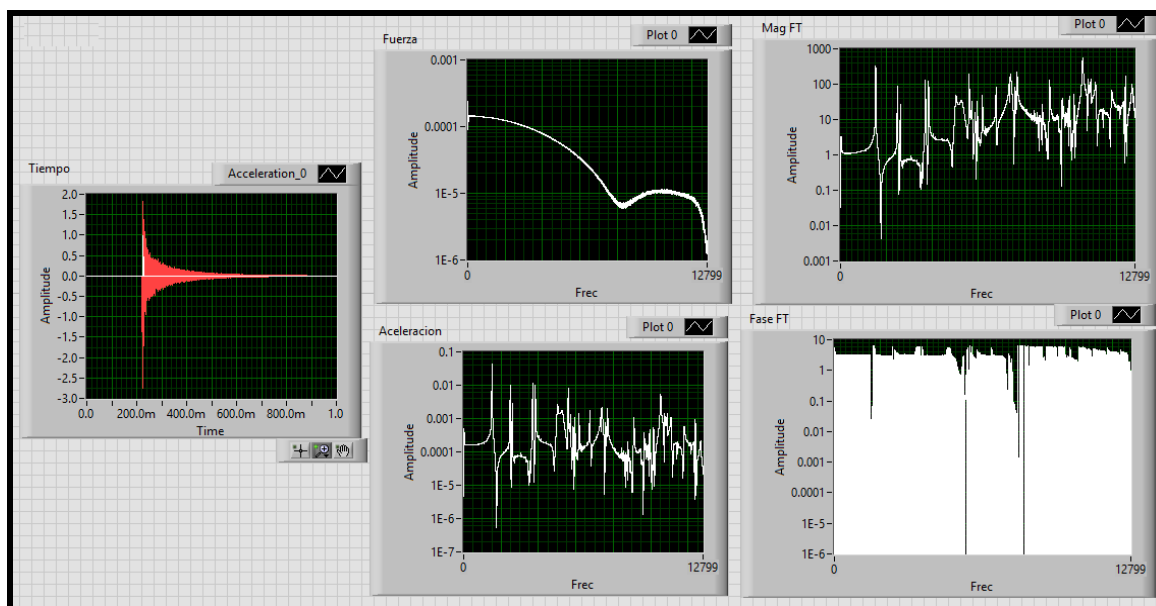
Figure 4. Spectral response of the transfer function magnitude "$G_{(1,1),(1,3)}$".
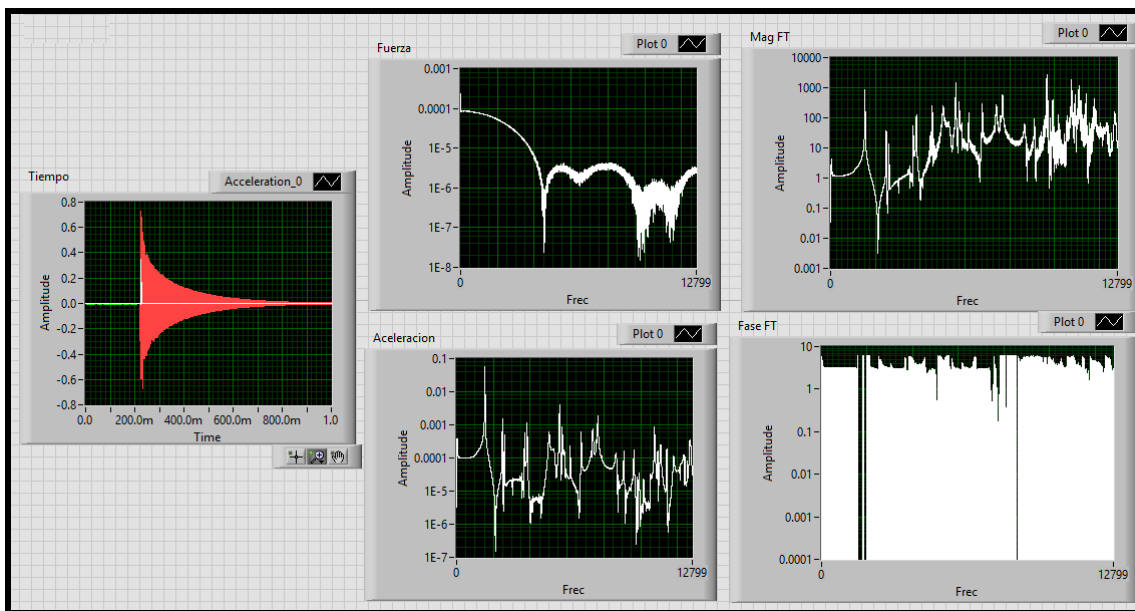
Figure 5. Spectral response of the transfer function magnitude "$G_{(2,3),(3,1)}$".
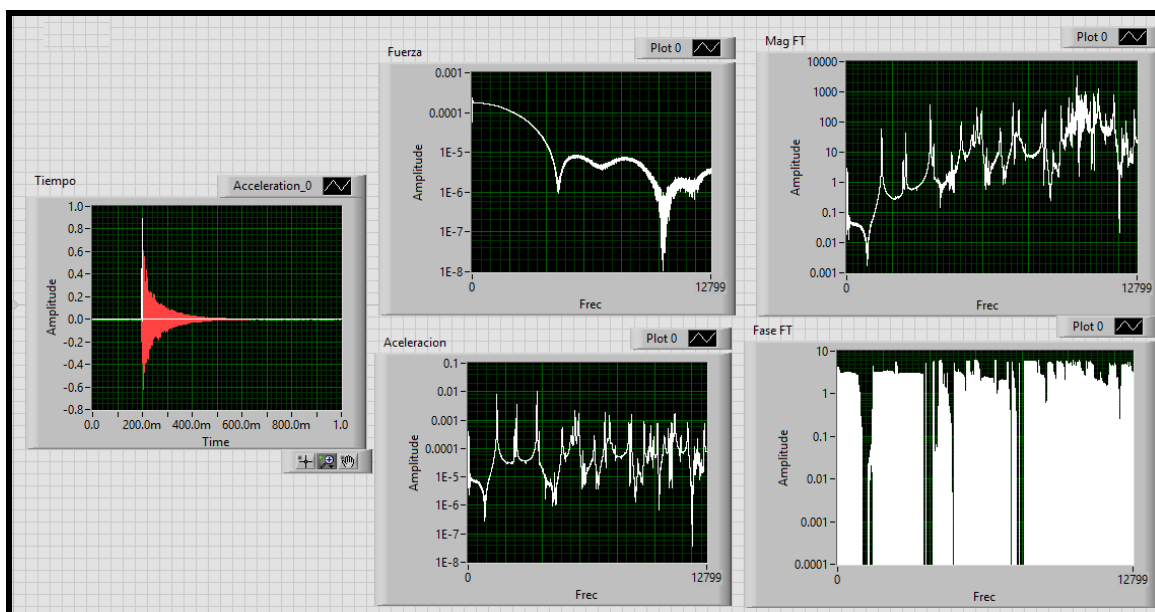
Figure 6. Spectral response of the transfer function magnitude "$G_{(1,2),(3,4)}$".
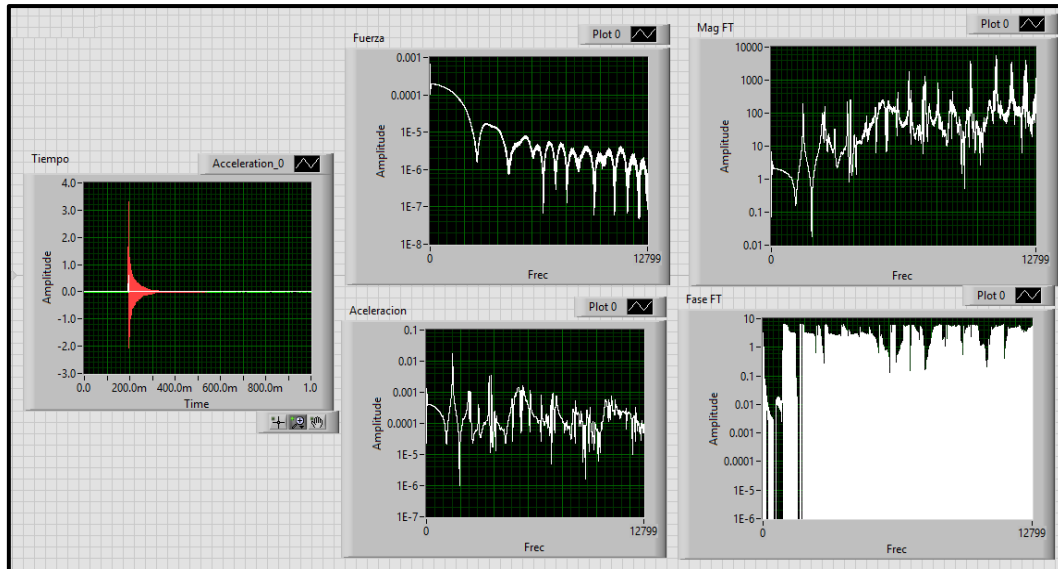
Figure 7. Spectral response of the transfer function magnitude "$G_{(1,4),(4,4)}$".

From the spectral response graphs the poles polynomial was gotten by analyzing the magnitude spectral peaks as well as Fig. 8 shows; therefore based on an average criteria from the 256 impact experiments, this 16th order polynomial was defined as:

$$P(\omega) = (2\pi[1500] - \omega)(2\pi[2400] - \omega)(2\pi[3700] - \omega)(2\pi[4200] - \omega)$$
$$(2\pi[5300] - \omega)(2\pi[6100] - \omega)(2\pi[6800] - \omega)(2\pi[7900] - \omega)$$
$$(2\pi[8100] - \omega)(2\pi[9400] - \omega)(2\pi[9600] - \omega)(2\pi[9800] - \omega)$$
$$(2\pi[10100] - \omega)(2\pi[10900] - \omega)(2\pi[11700] - \omega)(2\pi[12200] - \omega), \qquad (3)$$

In the same graphical criteria, but by analyzing the spectral minimum magnitude as well as it is shown on Fig. 9, in this experimental case for each transfer function the concerned zeros were defined as well as they are listed on Table 2.

Table 2. Model zeros list.

|	Z1	Z2	Z3	Z4	Z5	Z6	Z7	Z8	Z9	Z10	Z11	Z12
$Z_{(1,1)(1,1)}$	950	2500	3600	5300	7200	8300	9000	9600	10400	11300	12100	12600
$Z_{(1,1)(1,2)}$	850	1950	3100	3800	5000	9300	99000	10000				
$Z_{(1,1)(1,3)}$	1000	2000	3400	4400	7100	8900	10100	11800				
$Z_{(1,1)(1,4)}$	850	2100	3500	5900	7300	10100	11400					
$Z_{(1,1)(2,1)}$	750	2600	3700	5300	6600	7500	8300	9200	10500			
$Z_{(1,1)(2,2)}$	800	2100	5300	6700	8600	9200	10400	11500				
$Z_{(1,1)(2,3)}$	900	3100	5000	7200	8400	10200						
$Z_{(1,1)(2,4)}$	900	2000	3100	5200	6900	8300	9700					
$Z_{(1,1)(3,1)}$	800	4100	6300	7200	9300	10500						
$Z_{(1,1)(3,2)}$	900	4300	7000	8300	10100							
$Z_{(1,1)(3,3)}$	850	2900	5200	7300	10000	11300						
$Z_{(1,1)(3,4)}$	3800	6500	7100	9800	11300	12100						
$Z_{(1,1)(4,1)}$	4000	6200	7300	8400	9200	12000						
$Z_{(1,1)(4,2)}$	900	3900	5500	7100	9800							
$Z_{(1,1)(4,3)}$	3900	5300	7100	10100								
$Z_{(1,1)(4,4)}$	4200	7000	9300	12100								
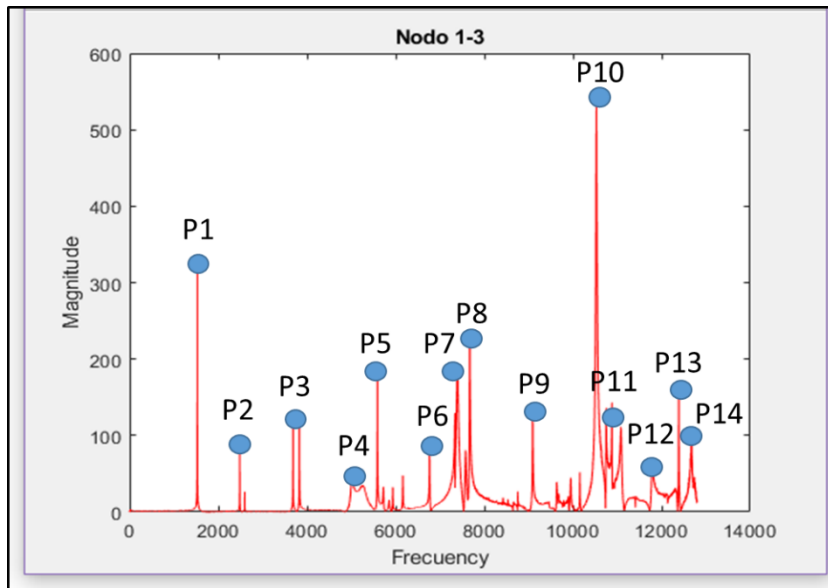
Figure 8. Graphical identification of the transfer function poles.
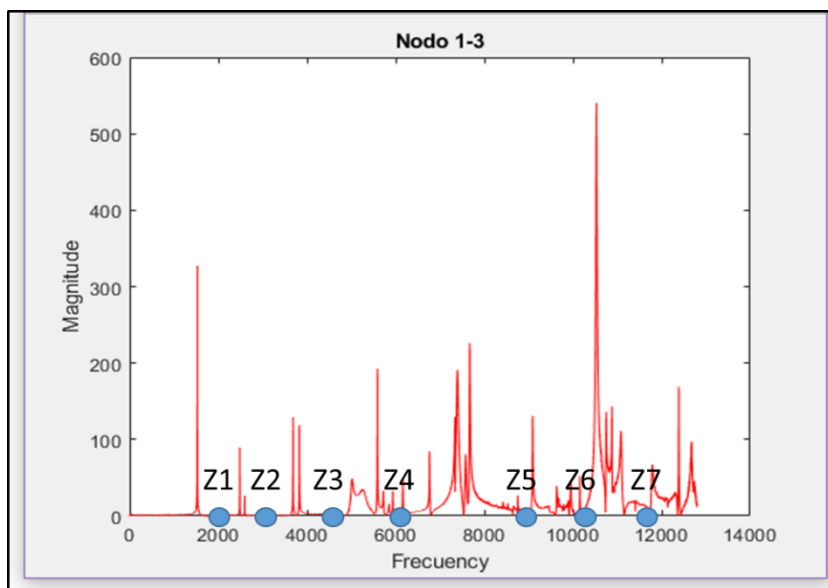

Figure 9. Graphical identification of the transfer fuction zeros.

The poles and zeros values estimation reported on Ec. 3 and Table 2 are similar than the ones estimated by the authors before, by applying others experimental techniques [17]. The bandwidth of the spectral range starts at 800 Hz and goes to 12600 Hz, because of the accelerometers limitations.

The transfer function response from an impulse input vector was simulated to compare the experimental data from the modal test with the numerical prediction in the frequency dominium. Based on the results plotted on Fig. 10 to 13, the simulation results are strongly accepted.

4. Air flow correlation and the model tuning

After the transfer function validation through its simulation and comparison with the experimental results, the set of blades shown on Fig. 1, was tested on a wind tunnel as it is illustrated on Fig. 14, with a set of air flow profiles with different turbulence ratio. The experimental results from the wind tunnel test are reported on Table 3.
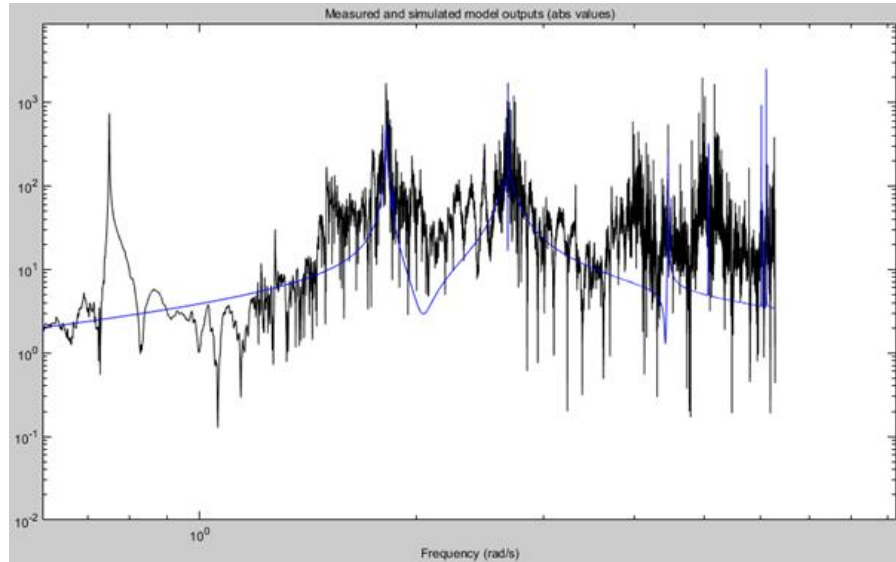
Figure 10. Spectral comparison between transfer function simulation and experimental results from "$G_{(1,1),(1,3)}$".
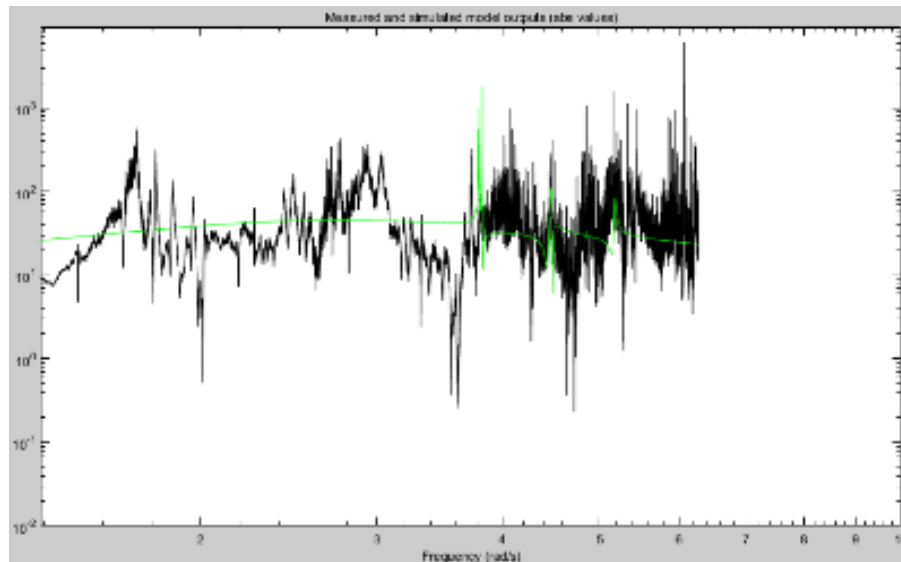
Figure 11. Spectral comparison between transfer function simulation and experimental results from "$G_{(2,3),(3,1)}$".
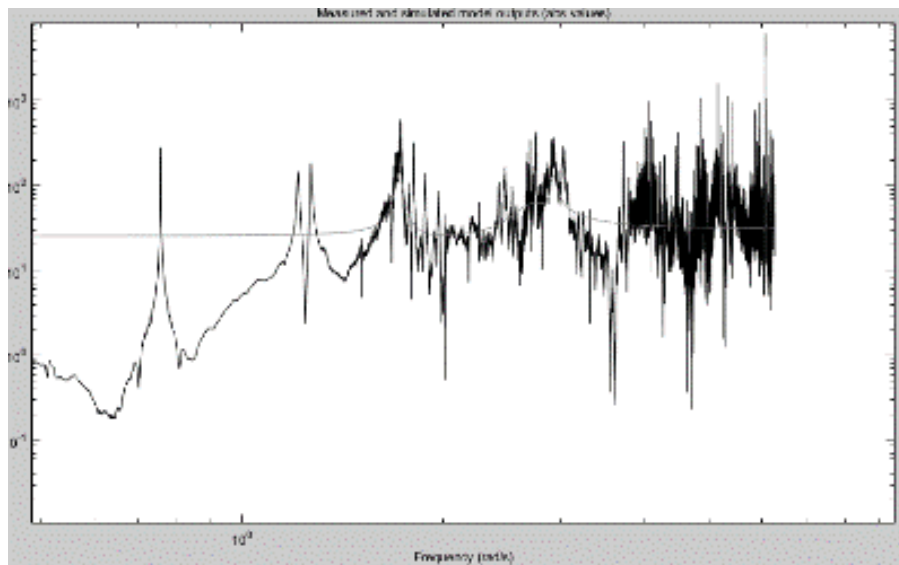
Figure 12. Spectral comparison between transfer function simulation and experimental results from "$G_{(1,2),(3,4)}$".
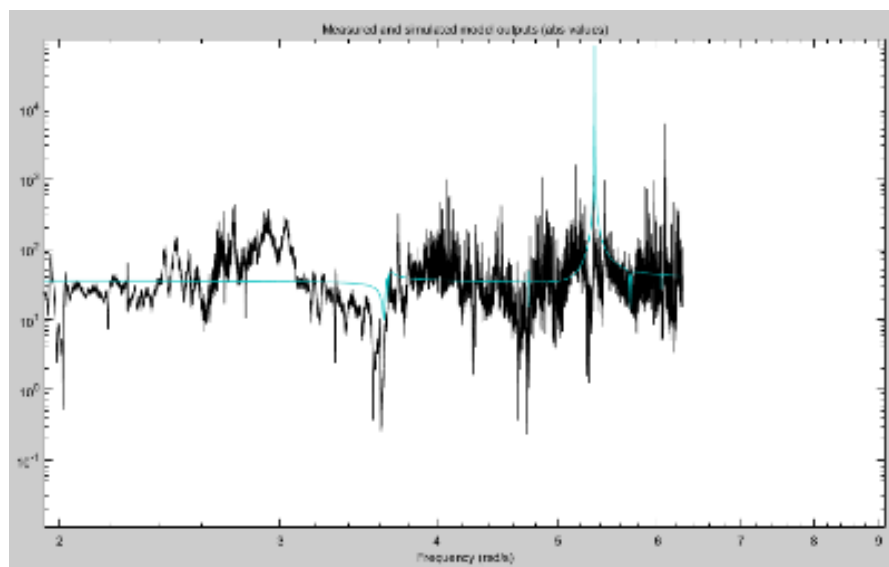
Figure 13. Spectral comparison between transfer function simulation and experimental results from "$G_{(1,4),(4,4)}$".
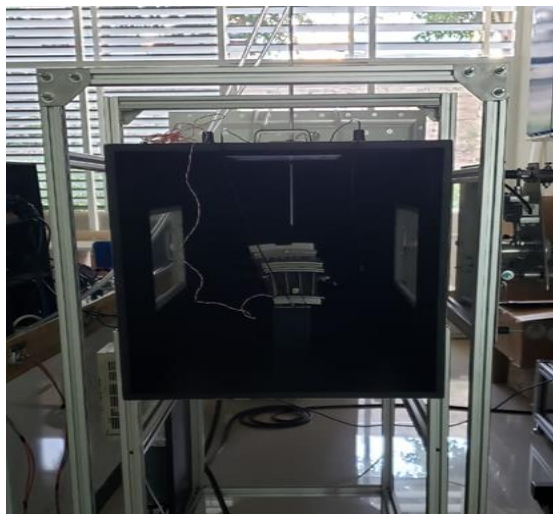
Figure 14. Experimental setup from the wind tunnel test".

Table 3. Summary of results from the wind tunnel test.

Turbulence Ratio	Resonance Vibrations RMS	Not Resonance Vibrations RMS
10 %	30.7 m/s^2	5.0 m/s^2
30 %	24.2 m/s^2	7.8 m/s^2
70 %	19.6 m/s^2	10.4 m/s^2

Resonance vibrations RMS and not resonance vibrations RMS values have been reported, because the hypothesis to analyze the turbulence ratio is based on the fact that due to the incident angle of the laminar air flow, it excites the resonance vibrations, while the not resonance vibrations are excited by the air flow turbulence.

5. Conclusions

By analyzing the plots from Figs. 10 to 13, the transfer function matrix from Ec. 1 has been experimentally validated, therefore; the dynamic order reduction from the complete model with 16 spatial degrees of freedom and 16th dynamic order, to the reduced model with the dynamic order defined by the zeros listed on Table 2, works correctly. Another fact that can be added to the last paragraph statement is that the transfer function matrix predicts the poles from Ec. 3 and zeros from Table 2, so that the spectral peaks that were not considered and taken out from the numerical prediction of Ec 1, are taken in account as not-resonance response of the vibrational model. Table 3 shows in certain level, the validation of the hypothesis which is based on the fact that due to the incident angle of the laminar air flow, it excites the resonance spectra from the set of blades, and the air flow turbulence excites the corresponded not resonance spectra. At the end, authors have developed and validated an instrumentation system that can predict the relationship between the laminar and turbulence air flow, incident in a set of blades. Specifically, in this case from a turbo-compressor stator, but than can be also implemented in heat interchangers grids from condenser or evaporators units from cooling systems, which works based on the vapor compression cooling cycle.

117

Acknowledgment

References

[1] M. Ponmurugan, M. Ravikumar, and A. Sundaramahalingam, "A review on utilization of waste heat from domestic refrigerator," Int. Conf. Mater. Manuf. Mach. 2019, vol. 2128, no. May 2015, p. 050015, 2019. https://doi.org/10.1063/1.5117987

[2] Global electricity prices in 2018, by selected country (in U.S. dollars per kilowatt hour). https://www.statista.com/statistics/263263/electricity-prices-in-selected-countries/.

[3] G. D. Librado, L. Alvaro, M. Santiyanes, and H. G. Cuatzin, "Dynamic Behavior Model for Cooling System Based on Vapor Compression Experimental Analysis and Simulation Validation Grounded on a Reduced Order Differential Equation with Few Degrees of Freedom," in ICONS 2018: The Thirteenth International Conference on Systems, 2018, no. c, pp. 57–62. https://www.thinkmind.org/download.php?articleid=icons_2018_4_20_48003

[4] K. Talukdar, "Modeling of Solar Photovoltaic Assisted Vapor Absorption Refrigeration System for Running an Ice Factory," IOSR J. Mech. Civ. Eng., vol. 14, no. 03, pp. 60–69, 2017. https://doi.org/10.9790/1684-1403016069

[5] The Vapor Compression Refriferation Cycle, Step by Step, Araner, February 2018, https://www.araner.com/blog/vapor-compression-refrigeration-cycle/

[6] M. Ahmad, A. Bontemps, H. Sallée, and D. Quenard, "Thermal testing and numerical simulation of a prototype cell using light wallboards coupling vacuum isolation panels and phase change material," Energy Build., vol. 38, no. 6, pp. 673–681, 2006. https://doi.org/10.1016/j.enbuild.2005.11.002

[7] H. Binici, O. Aksogan, M. N. Bodur, E. Akca, and S. Kapur, "Thermal isolation and mechanical properties of fibre reinforced mud bricks as wall materials," Constr. Build. Mater., vol. 21, no. 4, pp. 901–906, 2007. https://doi.org/10.1016/j.conbuildmat.2005.11.004

[8] S. L. Garrett, J. A. Adeff, T. J. Hofler, S. L. Garrett, J. A. Adeff, and T. J. Hoflers, "Thermoacoustics refrigerator for space application," J. Thermophys. Heat Transf., vol. 7, no. 4, pp. 595–599, 1993. https://doi.org/10.2514/3.466

[9] P. Gorria, J. L. Sánchez Llamazares, P. Álvarez, M. J. Pérez, J. Sánchez Marcos, and J. A. Blanco, "Relative cooling power enhancement in magneto-caloric nanostructured Pr2Fe17," J. Phys. D. Appl. Phys., vol. 41, no. 19, pp. 1–5, 2008. https://doi.org/10.1088/0022-3727/41/19/192003

[10] T. Moulton and G. K. Ananthasuresh, "Micromechanical devices with embedded electro-thermal-compliant actuation," Sensors Actuators, A Phys., vol. 90, no. 1–2, pp. 38–48, 2001. https://doi.org/10.1016/S0924-4247(00)00563-X.

[11] M. S. Layton and J. O'Hagan, Comparison of Alternate Cooling Technologies for California Power Plants:Economic, Environmental and Other Tradeoffs, 1st ed., vol. 2. Sacramento, California, 2002. http://large.stanford.edu/courses/2018/ph241/duboc2/docs/AR-1167.pdf.

[12] 2do Seminario Internacional del LaNITeF 2017, Publicaciones del Laboratorio Nacional de Investigación en Tecnologías del Frio, ISBN: 2594-2142X, Vol. 1, No. 2, 2017. https://www.cidesi.com/lanitef/index.html.

[13] M. Sakawa and T. Matsui, "Heat load prediction in district heating and cooling systems through recurrent neural networks," Int. J. Oper. Res., vol. 23, no. 3, pp. 284–300, 2015. https://doi.org/10.1504/IJOR.2015.069623

[14] A. Marwanto and S. Alifah, "Control of Air Cooling System Based on Fuzzy Logic," J. Telemat. Informatics, vol. 6, no. 1, pp. 63–70, 2018. https://doi.org/10.12928/jti.v6i1.

[15] E. E. Rodríguez-Vázquez, "Revista Internacional de Investigación e Innovación Tecnológica," Rev. Int. Investig. e Innovación Tecnológica, vol. 5, no. 30, pp. 1–9, 2018. https://doi.org/10.19053/20278306.v9.n2.2019.9154

[16] M. Stadler, W. Krause, M. Sonnenschein, and U. Vogel, "Modelling and evaluation of control schemes for enhancing load shift of electricity demand for cooling devices," Environ. Model. Softw., vol. 24, no. 2, pp. 285–295, 2009. https://doi.org/10.1016/j.envsoft.2008.07.003.

[17] H. J. Zúñiga, E. E. Rodríguez, L. A. Montoya, I. Mejia, C. Sandoval, "Vibrational modal model for a compressor blade," Rev. Int. Investig. e Innovación Tecnológica, vol. 7, no. 41, pp. 1–17, 2019. https://riiit.com.mx/apps/site/idem.php?module=Catalog&action=ViewItem&id=5039&item_id=85353&id=5039.

[18] G. Xu, J. Zhou, H. Geng, M. Lu, and W. Cheng, "Unbalance response analysis of the circumferential tie-rod combined rotor considering different support," in 2014 IEEE International Conference on Mechatronics and Automation, 2014, pp. 1323–1328. https://doi.org/10.1109/ICMA.2014.6885891

[19] A. Saxena, M. Chouksey, and A. Parey, "Effect of mesh stiffness of healthy and cracked gear tooth on modal and frequency response characteristics of geared rotor system," Mech. Mach. Theory, vol. 107, no. September 2016, pp. 261–273, 2017. https://doi.org/10.1016/j.mechmachtheory.2016.10.006

[20] B. Hu and H. Gharavi, "A Fast-Recursive Algorithm for Spectrum Tracking in Power Grid Systems," IEEE Trans. Smart Grid, vol. 10, p. 10.1109/TSG.2018.2813881, 2018. https://doi.org/10.1109/TSG.2018.2813881.